

Supporting Information

Self-Degrading Graphene Sheets for Tumor Therapy

Ievgen S. Donskyi, Ying Chen, Philip Nickl, Guy Guday, Haishi Qiao, Katharina Achazi, Andreas Lippitz, Wolfgang E.S. Unger, Christoph Böttcher, Wei Chen,* Mohsen Adeli,* and Rainer Haag**

Table of contents

Methods	2
Materials	6
Scheme S1.	6
Characterization	7
Figure S1.	7
Figure S2.	8
Table S1.	9
Table S2.	9
Table S3.	10
Figure S3.	11
Figure S4.	11
Figure S5.	12
Figure S6.	13
Figure S7.	14
Figure S8.	15
Figure S9.	15
Figure S10.	16
Figure S11.	17
Figure S12.	18
Figure S13.	19
Figure S14.	20
Table S4.	20
Figure S15.	21
References	21

Methods

X-ray photoelectron spectroscopy (XPS) experiments. Gold substrates used for analysis of graphene samples deposited thereon were cleaned in piranha solution (1:4) 30% H₂O₂: 98% H₂SO₄ (v/v) during ultrasonication at room temperature for 10 min. Then they were washed with the DI water 5 times and with acetone 2 times. After drying overnight, the studied compounds were dissolved in methanol and evenly distributed dropwise across the surface of gold substrates. XPS spectra were recorded using a Kratos Axis Ultra DLD spectrometer equipped with a monochromatized Al K α X-ray source (1486.69 eV) using an analyzer pass energy of 80 eV for survey spectra that were used for quantification. High-resolution, core-level O1s, C1s, and N1s spectra were recorded in FAT (fixed analyzer transmission) mode at a pass energy of 20 eV. Both the electron emission angle and the source-to-analyzer angle were 60°. The binding energy scale of the instrument was calibrated following a Kratos Analytical Ltd procedure that used ISO 15472 binding energy data. Spectra were recorded by setting the instrument to the hybrid lens mode and the slot mode, which provided approximately a 300 x 700 μm^2 analysis area and using charge neutralization. All XPS spectra were processed with the UNIFIT program (version 2017). A Gaussian/Lorentzian product function peak shape model GL (30) was used in combination with a Shirley background. If not otherwise denoted, the L-G mixing for component peaks in all spectra were constrained to the value of 0.39. Peak fitting of C1s spectra was performed by using an asymmetric peak shape model for the graphene C1s component peak and a symmetric peak shape model for all other component peaks. After peak fitting of the C1s spectra, all the binding energies were calibrated in reference to the graphene C1s component at a binding energy of 284.6 eV.

Near edge X-ray absorption fine structure (NEXAFS) experiments: NEXAFS measurements were carried out at the synchrotron radiation source BESSY II (Berlin, Germany) at the HE-SGM monochromator dipole magnet CRG beamline. NEXAFS spectra were acquired in total energy electron yield (TEY) mode using a channel plate detector. The resolution $E/\Delta E$ of the monochromator at the carbonyl π^* resonance ($h\nu = 287.4$ eV) was in the order of 2500. Raw

spectra were divided by ring current and monochromator transmission, the latter obtained with a freshly sputtered Au sample.^[1] Alignment of the energy scale was achieved by using an I_0 feature referenced to a $C1s \rightarrow \pi^*$ resonance at 285.4 eV measured with a fresh surface of HOPG (highly ordered pyrolytic graphite, Advanced Ceramic Corp., Cleveland, USA).^[2] If not otherwise denoted, all NEXAFS spectra are shown after subtraction of the pre-edges followed by normalization of the post-edge count rates to one.^[1] All C K-edges were measured at 55° incident angle of the linearly polarized synchrotron light beam.

CCK8 assay. CCK8 assays were performed using a TECAN Infinite M200 Pro microplate reader at the wavelengths of 562 nm and 450 nm. All cell experiments were conducted according to German genetic engineering laws and German biosafety guidelines in the laboratory (level 1). Dulbecco modified eagle's medium and fetal bovine serum were used for all following experiments. HeLa cells (ACC 57) were obtained from Leibniz-Institut DSMZ - Deutsche Sammlung von Mikroorganismen und Zellkulturen GmbH and cultured in Dulbecco's Modified Eagle Medium (DMEM) supplemented with 2% glutamine, 100 U/mL penicillin, 100 µg/mL streptomycin (all from Gibco BRL, Eggenstein, Germany), and 10% fetal calf serum (Biochrom AG, Berlin, Germany). The cells were incubated in a humidified atmosphere with 5% CO₂ at 37 °C. For CCK8 assays, HeLa cells (10⁴ cells per well) were seeded in 96-well plates with 100 µL DMEM and incubated for 24 h before the tests. nG_{DOX}-Trz, nG-G-M, and nG_{DOX}-G-M were added to the 96-well plates with different concentrations and incubated for another 48 h. NIR irradiation experiment was performed at similar conditions after incubation with cells for 2 hours by 10 min irradiation using NIR laser (808 nm, 1 W/cm²). After the cell culture medium solutions were removed, the cells were rinsed with PBS twice. 100 µL culture medium with 10 µL CCK8 solution was added to each well. After incubation for 2 hours, 50 µL medium was transferred to a new plate and the absorption was measured at a wavelength of 450 nm using the microplate reader. Cells without any treatments were regarded as a negative control.

Fluorescence measurements. Fluorescence measurements were performed on a Jasco FP-6500 fluorometer in the range of 500-750 nm. MilliQ quality water was used for all experiments. Measurements were performed in quartz cuvettes. Width of the excitation and emission bands varied between 3 and 5 nm and the excitation wavelength was set to 498 nm.

UV-Vis measurements. UV-Vis absorption spectra were recorded using standard 10x10 mm optical PMMA cuvettes and the UV-Vis spectrophotometer Cary 8454 with diode array system manufactured by Agilent, USA. The absorption spectra were recorded in the wavelength regime of 400 – 800 nm. PBS water was used for blank measurements.

Confocal laser scanning microscopy (CLSM). CLSM was performed using a Leica TCS SP8 with 63 x oil-immersion objective lens and Leica Confocal Software (LAS X) for image processing. Images were taken in the sequential mode using two sequences. In sequence one, the fluorescence signal of Hoechst 33342 (Hoechst channel; excitation 405nm, emission: 416nm - 478nm) and sequence two the fluorescence signal of doxorubicin (DOX channel: excitation 488nm, emission 522nm - 699nm). Transmitted light images were taken in sequence one using the 405 nm laser as light source. For sample preparation, HeLa cells cultured as described above, were seeded in 8 Well ibiTreat μ -Slides (ibidi GmbH, Martinsried, Germany) at a concentration using 3×10^4 cells per well. After incubation for 24 h, nG_{DOX}-G-M in deionized water at concentration of 0.1 μ g/mL was added to the cells for 3 hours at 37 °C. Cell nuclei were stained applying 1 μ g/ml Hoechst 33342 (Life Technologies GmbH, Darmstadt, Germany) for 20 min. Afterwards, cell culture medium was removed, and the cells were rinsed with PBS and fresh cell culture medium was added for imaging.

In Vitro Stability Experiments. 10 μ L solutions of nG-G-M were mixed with PBS (pH 6.5), CB (50 μ M) and NaCl (150 mM). Solutions were left for different time periods at 25 °C or 37 °C. 30 minutes before the UV measurements 5 mM glucose was added to start the enzymatic reactions.

Release experiments. To investigate the release of DOX from nG_{DOX}-G-M, material was dispersed in the PBS buffer solutions in the presence of glucose (5.0 mM), NaCl (150 mM), at pH 5.6 and 7.4. The fluorescence of the samples in the quartz cuvettes was recorded after 0.5, 1, 1.5, 2, 3, 4, and 5 hours and the maximum of the emittance at 593 nm was used for further calculations of the drug release. To determine the overall loading, nG_{DOX}-G-M was sonicated to separate DOX from graphene sheets, supernatant was collected, and its fluorescence was measured.

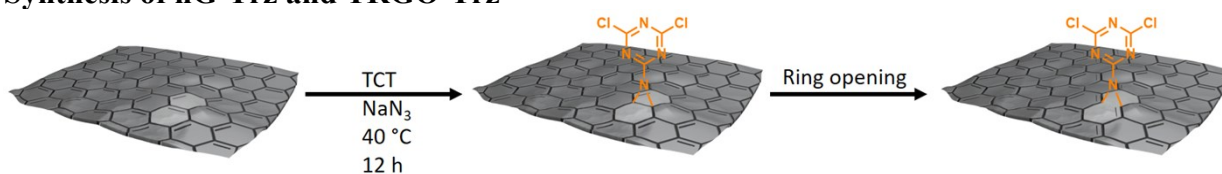
Tumor models on nude mice. Female BALB/c nude mice (four weeks old) were purchased from Model Animal Research Center of Nanjing University (Nanjing, China), and all animal experiments were conducted in compliance with the National Institute of Health Guide for the Care and Use of Laboratory Animals (China). 1×10^6 HeLa cells were subcutaneously inoculated into the right flank of one nude mouse to construct the tumor-bearing mice. Tumor size was measured by electronic caliper, the tumor volume (V) was calculated as $V = a^2 \times b / 2$ (a and b represent the width and length of the tumor, respectively), and the body weight of nude mice was recorded by an electronic balance.

Immunohistochemistry. Tumors were fixed with 4% paraformaldehyde solution, embedded in paraffin and the samples were cut into 4 μ m-thick sections. Slides were stained using anti-Cleaved Caspase-3 antibody (Cell signaling, clone Asp175) and anti-Ki-67 (Cell signaling, clone 8D5) at 1:100 dilution on a Leica Bond automated immunohistochemistry staining platform, followed by staining with DAB (DAKO, K5007, rat HRP, 1:100) for tumors. For the latter, the cell nucleus was stained with hematoxylin. Slides were imaged on an inverted fluorescence microscope using the digital microscope (ECLIPSE Ci-L, Nikon, JAPAN) and quantification was performed by analyzing 10 randomly selected images per slide using ImageJ.

Materials

Graphite powder (median diameter 7-10 microns) was purchased from ACROS Organics. Thermally reduced graphene oxide (TRGO) with the average size of graphene sheets around 300-400 nm was prepared according to published procedure and provided by R. Mülhaupt et al.^[3] Sodium hypochlorite (11-14% available chlorine), phosphate buffer solution 1.0 M, pH 7.4 (25 °C), 1-methyl-2-pyrrolidinone (NMP) (99.5%), celestine blue (dye content 80 %), glucose oxidase were purchased from Sigma Aldrich and used directly without further purification. Myeloperoxidase was purchased from Planta Natural Products. 2,4,6-trichloro-1,3,5-triazine (TCT) (99%), triethylamine (TEA), and sodium azide (NaN_3) (99%) were purchased from Acros Organics. Anhydrous solvents were either obtained from solvent purification (MBraun MB-SPS-800) system or purchased as ultra-dry solvents from Acros Organics. Cell counting kit-8 (CCK8) assay was purchased from Thermo Fisher Scientific. Deionized water was applied in all experiments. Water was derived from a Milli-Q advantage A10 water purification system in all experiments. Biotech cellulose ester dialysis bags MWCO 300 kDa were purchased from Spectrum labs. All chemical compounds were used without further purification.

Synthesis of nG-Trz and TRGO-Trz



Scheme S1. Schematic representation of the functionalization of different graphene platforms.

Characterization

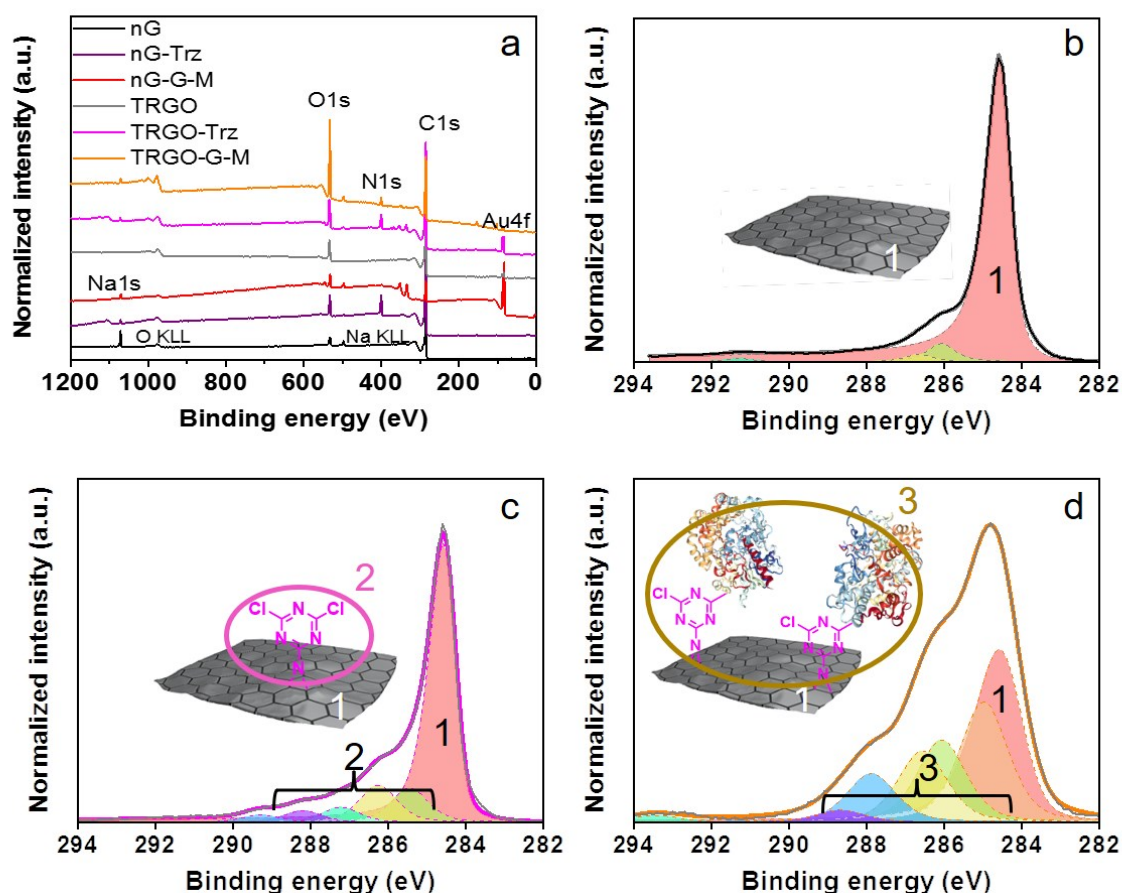


Figure S1. (a) Survey spectra of nG, nG-Trz, nG-G-M, TRGO, TRGO-Trz, TRGO-G-M. Au4f signal originates from the substrate. (b) Highly resolved C1s XPS spectra of (b) TRGO, (c) TRGO-Trz, and (d) TRGO-G-M. C1s XPS spectra of nG, nG-Trz, and nG-G-M are shown in the main text, Figure 1. For further XPS assignments see Table S2.

The survey spectra of all materials are shown in Figure S1a. Relative element fractions are listed in Table S1. The decrease in C/O ratio on different functionalization steps showed successful conjugation of triazine moieties and enzymes to the surface of graphene sheets. The component 1 in the C1s spectra of TRGO derivatives is attributed to C=C bonds of graphene. Components under the bracket 2 in the C1s spectra of TRGO-Trz (Figure 1c) are attributed to conjugated triazine groups on the graphene sheets. A significant change in the C1s spectra of TRGO-G-M

corresponded to the enzymes that are conjugated to the surface of TRGO-Trz, similar to the nG-G-M (Figure 1 in the main text).

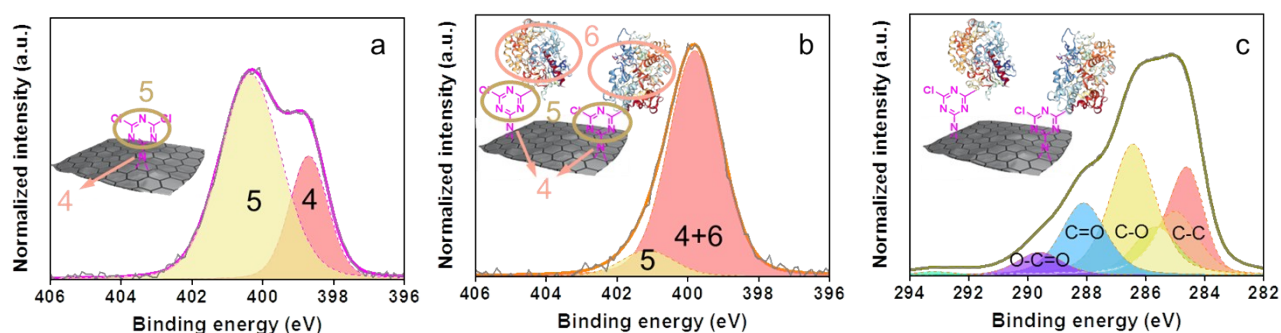


Figure S2. Highly resolved N1s XPS spectra of (a) TRGO-Trz and (b) TRGO-G-M respectively, with peak fittings. c) Highly resolved C1s XPS spectra of TRGO-G-M after enzymatic reaction. For further XPS assignments see Table S2.

Similar N1s spectra of nG-Trz and TRGO-Trz (Figure S2a, S2b) as well as nG-G-M and TRGO-G-M (Figure S2c, S2d) showed high reproducibility of the functionalization of different graphene sheets.

Table S1. Relative element fractions and C/O atomic ratio obtained by quantification of the XPS spectra displayed in Figure S1a.

Sample	C at%	N at%	C/O ratio
nG	92.5	n.d.	14.9
nG-Trz	75.9	14.8	9.6
nG-G-M	65.6	4.2	3.4
TRGO	92.0	n.d.	12.6
TRGO-Trz	80.9	7.7	8.7
TRGO-G-M	68.1	4.2	3.2
TRGO-G-M (after reaction)	63.2	8.1	2.9

Table S2. Spectroscopic parameters of XPS spectra of nG, TRGO, nG-trz, TRGO-Trz, nG-G-M, and TRGO-G-M, which were obtained by peak fitting using the UNIFIT 2017 software.

Sample	Spectrum	Binding energy	L-G Mixing	FWHM	Interpretation	Relat. Area	Abs. Area
nG	C 1s	284.6	0.39	0.6	C-C sp ²	0.92	36066
		285.6	0.39	0.8	C-O-C	0.04	1635
		286.4	0.39	0.8	C-O-H	0.03	987
		291.4	0.39	0.8	π - π^* shake ups	0.01	500
TRGO	C1s	284.6	0.39	0.8	C-C sp ²	0.80	29348
		285.4	0.39	1.0	C-O-C	0.10	3521
		286.3	0.39	1.0	C-O-H	0.08	2851
		291.3	0.39	1.0	π - π^* shake ups	0.01	312
nG-Trz	C1s	284.6	0.39	0.6	C-C sp ²	0.66	16388
		285.4	0.39	0.8	C-N=C	0.11	2706
		286.1	0.39	0.8	C-O	0.10	2428
		286.8	0.39	0.8	C-Cl	0.07	1631
		287.8	0.39	0.8	NH-C=O	0.03	908
		288.6	0.39	0.8	O-C=O	0.03	884
	N1s	398.9	0.42	1.2	C-N-C	0.25	2913
		400.5	0.42	2.0	C-N=C, N-C=O	0.75	7451
TRGO-Trz	C1s	284.6	0.39	0.8	C-C sp ²	0.68	26847
		285.4	0.39	1.1	C-N=C	0.10	4093
		286.3	0.39	1.1	C-O	0.11	4480
		287.2	0.39	1.1	C-Cl	0.05	1810
		288.2	0.39	1.1	NH-C=O	0.04	1395
		289.3	0.39	1.1	O-C=O	0.02	873
	N1s	398.7	0.42	1.2	C-N-C	0.27	1978
		400.3	0.42	2.0	C-N=C, N-C=O	0.73	5245
nG-G-M	C1s	284.6	0.39	1.23	C-C sp ²	0.29	3004
		285.0	0.39	1.23	C-C aliphatic	0.36	3619

		286.2	0.39	1.23	C–N	0.18	1876
		287.2	0.39	1.23	C–O	0.09	952
		288.4	0.39	1.23	NH–C=O	0.05	488
		289.9	0.39	1.23	O–C=O	0.02	146
		292.7	0.39	1.23	π – π^* shake ups	0.01	99
	N1s	399.5	0.42	1.4	C–N–C	0.89	480
		400.7	0.42	1.4	C–N=C, N– C=O	0.11	62
TRGO-G-M	C1s	284.6	0.39	1.48	C–C sp^2	0.34	5767
		285.0	0.39	1.48	C–C _{aliphatic}	0.23	3841
		286.1	0.39	1.48	C–N	0.16	2637
		286.5	0.39	1.48	C–O	0.14	2288
		287.9	0.39	1.48	NH–C=O	0.09	1561
		288.7	0.39	1.48	O–C=O	0.02	385
		293.4	0.39	1.48	π – π^* shake ups	0.01	205
	N1s	399.8	0.42	1.7	C–N–C	0.85	1575
		400.8	0.42	1.7	C–N=C, N– C=O	0.15	284
TRGO-G-M (after reaction)	C1s	284.6	0.39	1.51	C–C sp^2	0.22	5200
		285.0	0.39	1.81	C–C _{aliphatic}	0.15	3461
		285.7	0.39	1.81	C–N	0.11	2640
		286.4	0.39	1.81	C–O	0.30	7124
		288.1	0.39	1.81	NH–C=O	0.17	3949
		289.6	0.39	1.81	O–C=O	0.05	1274
		293.1	0.39	1.81	π – π^* shake ups	0.01	196

Table S3. Resonances in the C K-edge NEXAFS for nG, TRGO, nG-trz, TRGO-Trz, nG-G-M, and TRGO-G-M.

Sample		Photon energy	Assignment
nG	a	285.3 ^[2,4]	C1s \rightarrow π^* (C=C)
	b	288.6 ^[5]	C1s \rightarrow σ^* (C–O)
TRGO	a'	285.4 ^[2,4]	C1s \rightarrow π^* (C=C)
	a	285.3 ^[2,4]	C1s \rightarrow π^* (C=C)
nG-Trz	c	288.1 ^[6,7]	C1s \rightarrow σ^* (C–N)
	d	289.3 ^[6,7]	C1s \rightarrow σ^* (C–N)
TRGO-Trz	a	285.3 ^[2,4]	C1s \rightarrow π^* (C=C)
	c	288.1 ^[6,7]	C1s \rightarrow σ^* (C–N)
	d	289.3 ^[6,7]	C1s \rightarrow σ^* (C–N)
	a	285.3 ^[2,4]	C1s \rightarrow π^* (C=C)
nG-G-M	b'	288.5 ^[8]	C1s \rightarrow π^* (C–H)
	a	285.0 ^[2,4]	C1s \rightarrow π^* (C=C)
TRGO-G-M	b''	288.1 ^[8]	C1s \rightarrow π^* (C–H)

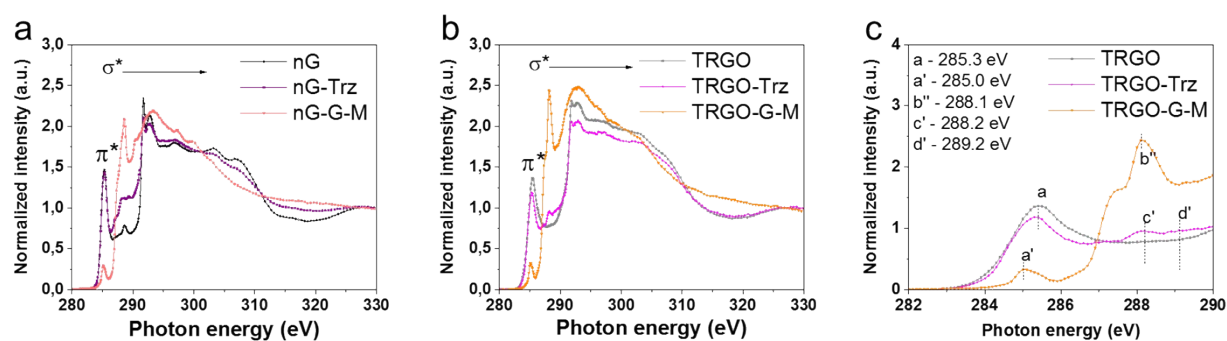


Figure S3. (a) C K-edge NEXAFS of (a) nG, nG-trz, nG-G-M, (b) C K-edge NEXAFS and (c) expanded C K-edge NEXAFS of TRGO, TRGO-Trz, TRGO-G-M. For assignments see Table S3.

NEXAFS was used as a method for the characterization of the surface of synthesized graphene derivatives (Figure 1, Figure S3 and Table S3). The spectra of both types of graphene sheets (nG and TRGO) showed similar resonances at different steps of functionalization. This result proved comparable coverage of the nG and TRGO sheets with triazine moieties and enzymes.

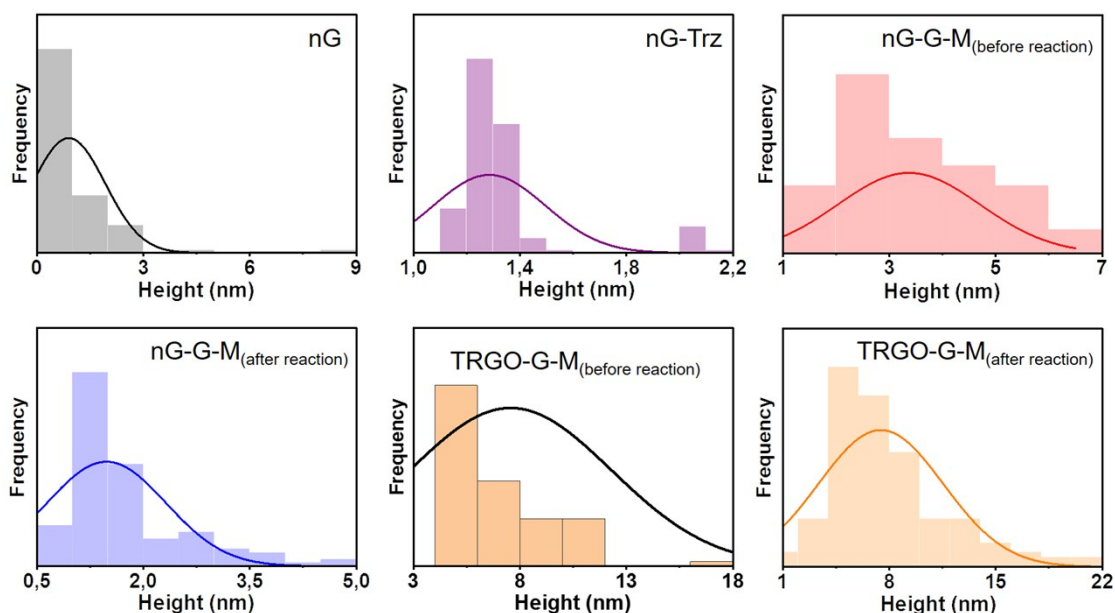


Figure S4. AFM height histograms for nG, nG-Trz, nG-G-M (before and after enzymatic reaction) and TRGO-G-M (before and after enzymatic reaction).

The height of graphene sheets increased after each functionalization step, as shown on Figure S6 and Table 1. This is another indicator for the successful conjugation of triazine moieties and enzymes to the surface of graphene sheets.

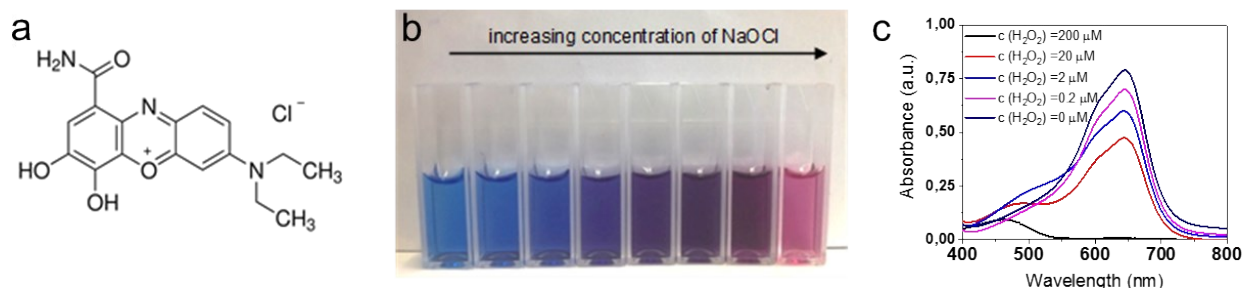


Figure S5. (a) Structural formula of celestine blue used as indicator for the enzymatic activity of graphene derivatives and their ability to produce NaOCl. (b) Color of celestine blue solutions at different concentrations of NaOCl (0, 10, 20, 30, 40, 50, 60, and 70 μM from left to right). (c) UV-Vis absorption spectra of CB after incubation with different concentrations of H_2O_2 (0, 0.2, 2, 20, 200 μM from up to down) in the presence of MPO and sodium chloride at pH 5.6.

To study the enzymatic activity of nG-G-M and TRGO-G-M, celestine blue (CB) was used as an indicator. CB is a sensitive dye towards oxidation by NaOCl, whereas no reaction occurs in presence of H_2O_2 in the investigated concentration range. At the same time in the presence of MPO the oxidation of the dye was already observed at a 0.2 μM concentration of H_2O_2 . Depending on the amount of NaOCl, its color changes from blue towards purple and yellow, as shown in Figure S5.

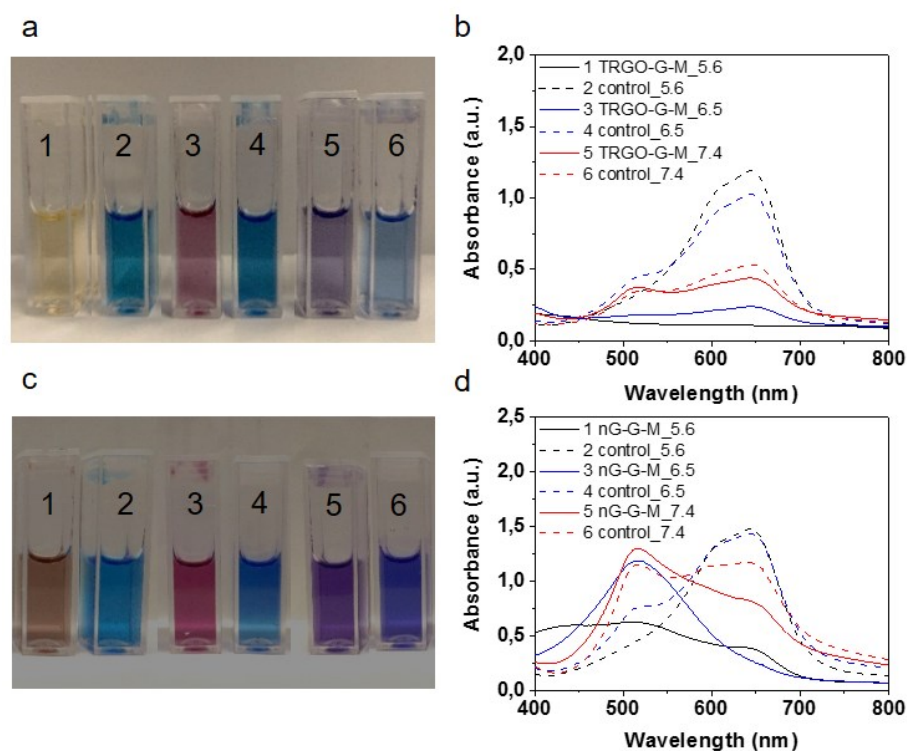


Figure S6. (a) Photo of PBS solutions containing 5 mM glucose and CB after mixing with 50 μ l of TRGO-G-M at different pH values (cuvettes 1 (5.6), 3 (6.5), and 5 (7.4), respectively) as well as control PBS solutions without graphene derivatives (cuvettes 2, 4, and 6, respectively). (b) UV-Vis absorption spectra of CB after incubation with TRGO-G-M at pH 5.6, 6.5, and 7.4 (solid lines) and control PBS solutions without graphene derivatives (dashed lines). (c) PBS solutions containing glucose and CB after mixing with 50 μ l nG-G-M at different pH values (cuvettes 1 (5.6), 3 (6.5), and 5 (7.4), respectively) as well as control PBS solutions without graphene derivatives (cuvettes 2, 4, and 6, respectively). (d) UV-Vis absorption spectra of CB after incubation with nG-G-M at pH 5.6, 6.5, and 7.4 (solid lines) and control PBS solutions without graphene derivatives (dashed lines).

The enzymatic production of NaOCl by nG-G-M and TRGO-G-M was studied in the presence of glucose (5.0 mM), NaCl (150 mM), and CB (50 μ M) at pH 5.6, 6.5, and 7.4. All samples were stored at room temperature and the color change of CB was followed by UV-Vis absorption spectroscopy. For each pH value, solutions containing CB, NaCl, and glucose were prepared as control experiments. After incubation of CB with nG-G-M and TRGO-G-M, their colors were

significantly bleached at acidic pH. Also, the maximum absorption wavelength of CB shifted from 650 nm to 520 nm. This result indicated a high amount of produced NaOCl by nG-G-M and TRGO-G-M and the highest enzymatic activity at pH 5.6.

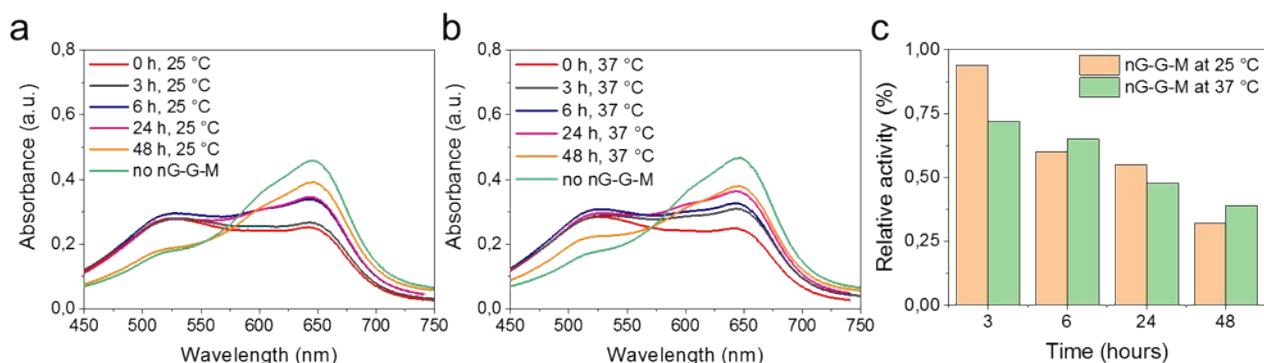


Figure S7. (a, b) UV-Vis absorption spectra of CB after incubation with nG-G-M at pH 6.5 at 25 °C and 37 °C respectively for different time intervals and control CB solution without nG-G-M. c) Graph of relative activity of nG-G-M, showing in vitro stability of the nG-G-M after different incubation times

To evaluate in vitro stability of nG-G-M, the enzymatic production of NaOCl by 10 μ l of this compound was studied at different time-frames and different temperatures in the presence of NaCl (150 mM), CB (50 μ M) at pH 6.5. Glucose (5 mM) was added 30 minutes before the UV measurements. Relative activity was calculated according to the relative decrease of the UV peak intensity at 650 nm for different time-frames in comparison with non-treated by nG-G-M sample and a sample, where nG-G-M was added 30 minutes before the UV measurements.

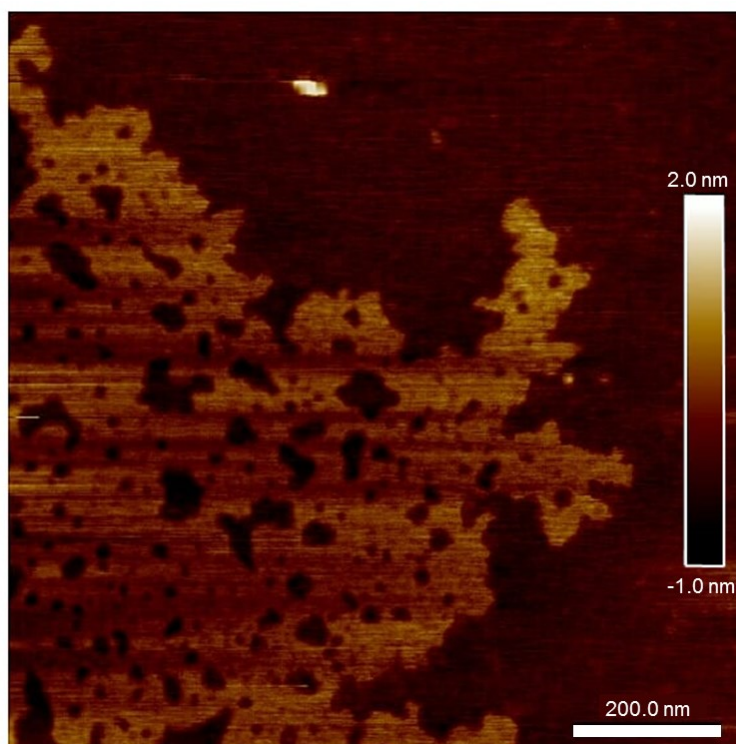


Figure S8. AFM image of graphene flake incubated with concentrated solution of NaOCl after separation of oxidized small sheets. Scale bar corresponds to 200 nm.

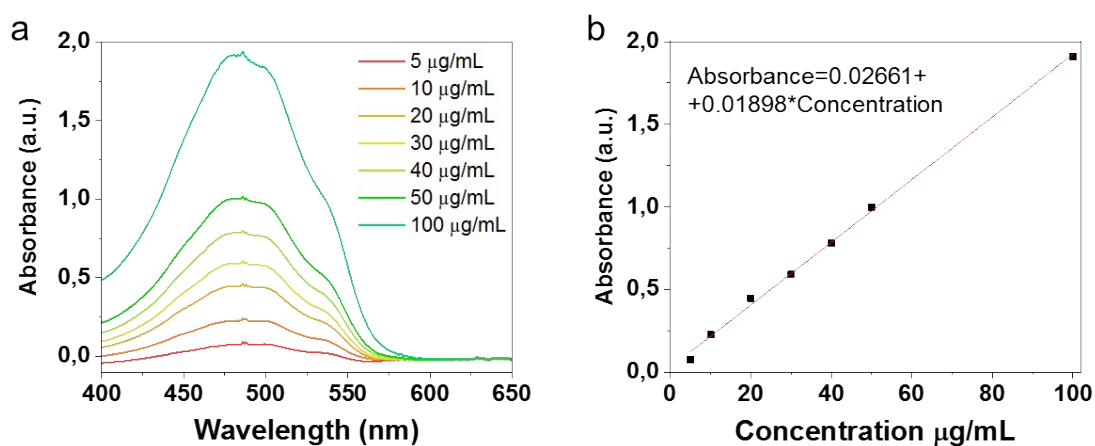


Figure S9. (a) UV spectra of different concentrations of doxorubicin. (b) Calibration curve of doxorubicin based on maximum absorbance peak at 480 nm.

To determine the loading capacity of nG_{DOX}-Trz using UV-Vis absorption spectroscopy, nG-Trz (2 mg*mL⁻¹) was mixed with DOX*HCl (4 mg*mL⁻¹) and TEA (0.065mL) in DMSO solution and

stirred for 20 h at 4 °C. Then the product was purified by centrifugation and the loading capacity was calculated according to Equation 1.

$$\text{Loading capacity [wt - \%]} = \frac{(c_1 - c_2) * v}{m_{nG}} \quad \text{Equation 1}$$

Where, c_1 and c_2 describe the concentrations of doxorubicin before and after incubation, v represents the total volume of the mixture and m_{nG} the mass of nanographene. Therefore, the value of loading capacity was calculated to be 106 ± 1 wt% for nG_{DOX} -Trz.

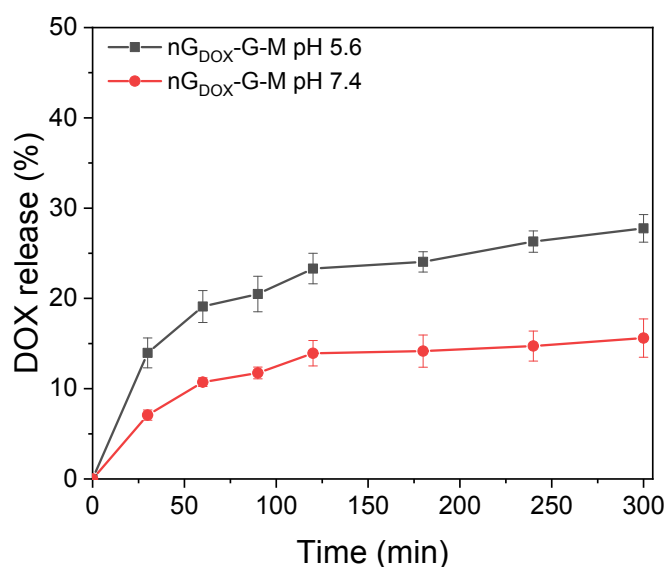


Figure S10. Drug release profile of nG_{DOX} -G-M at different pH values.

DOX showed higher release in acidic pH, due to the increased rate of the NaOCl formation, in comparison with a release profile at neutral pH.

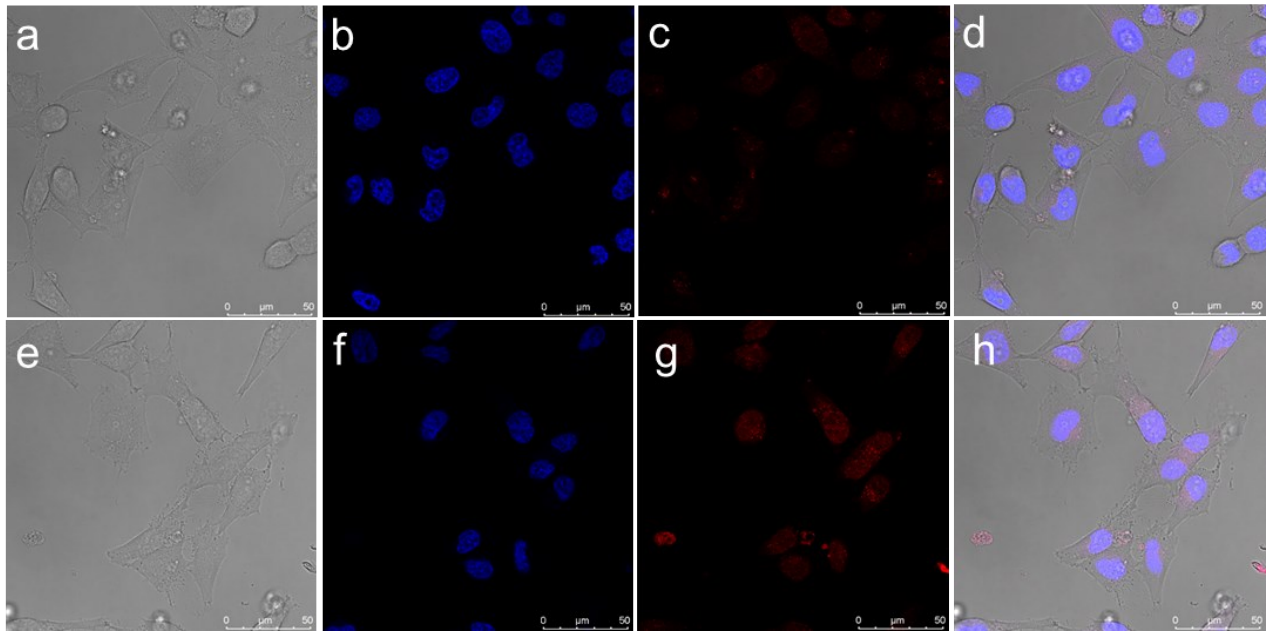


Figure S11. Confocal laser scanning microscopy images of (a-d) non-treated HeLa cells and (e-h) HeLa cells after 3 hours of incubation with nG_{DOX}-G-M. From left to right: transmitted light channel, Hoechst channel, DOX channel and overlay images. Hoechst 33342 was used to stain the nucleus shown in blue, the fluorescence signal of DOX is shown in red. Scale bars correspond to 50 μm .

The cellular uptake of doxorubicin was studied for HeLa cells using confocal laser scanning microscopy. Localization of doxorubicin in the nucleus of HeLa cells was observed after 3 hours of incubation with nG_{DOX}-G-M at a concentration of 0.1 $\mu\text{g}/\text{mL}$.

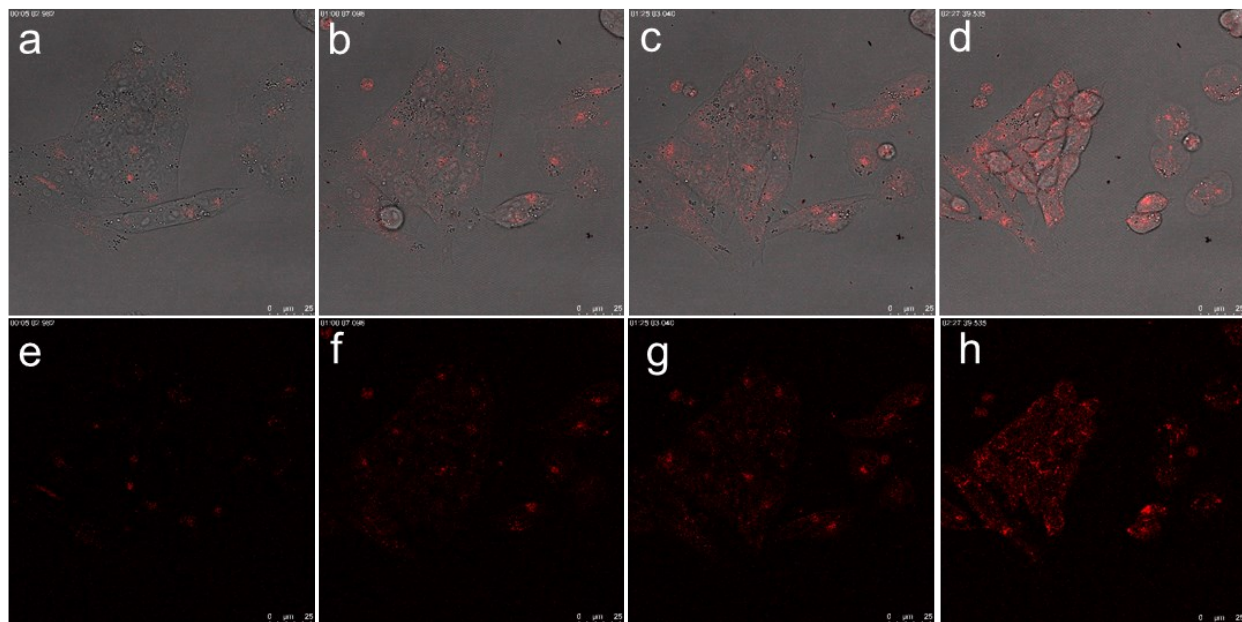


Figure S12. Confocal laser scanning microscopy images obtained using live tracking experiment of (a-d) overlay channel and (e-h) DOX channel of HeLa cells after different time points (5 minutes, 1 hour, 2 hours, 2.5 hours) of incubation with nG_{DOX} -G-M. Scale bars correspond to 25 μm .

Live tracking experiment was performed on a same area of the cells, so that the uptake of the DOX was possible to track in time. Increase in the intensity of the drug inside the cells clearly shows increased uptake of a drug through the time of the experiment.

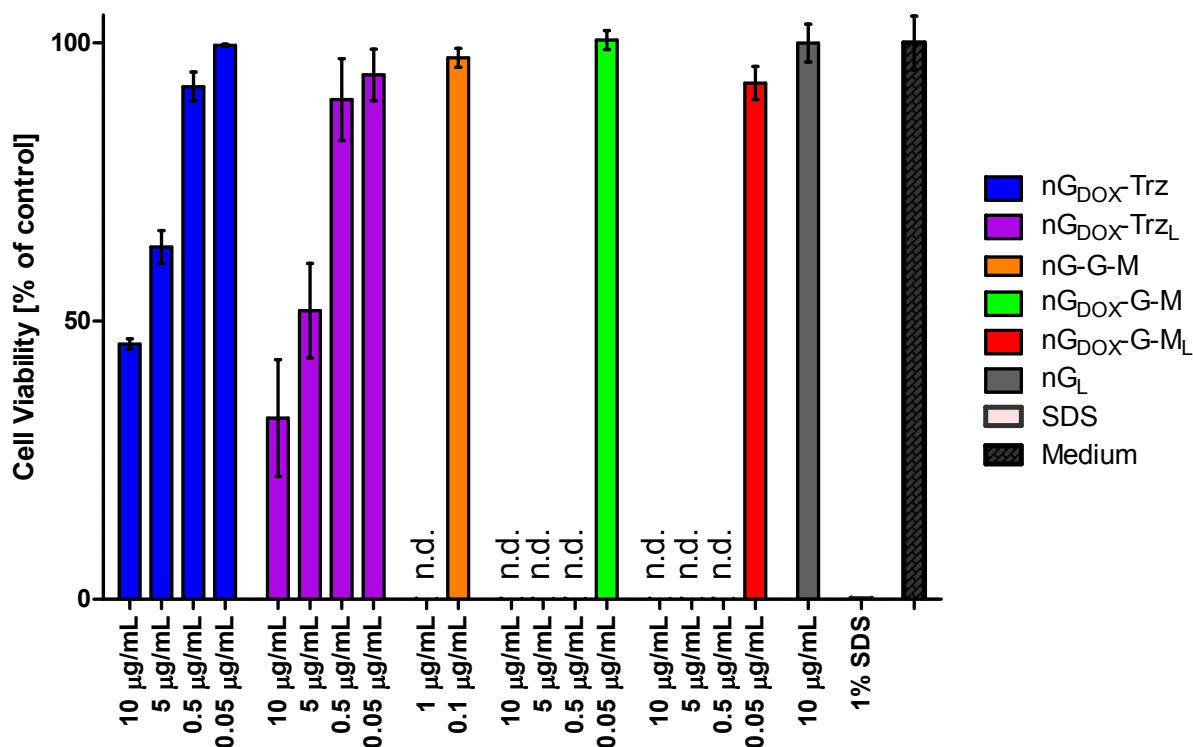


Figure S13. Cell viability of HeLa cells obtained by the CCK-8 assay. HeLa cells were treated with nG, nG_{DOX}-Trz, nG_{DOX}-G-M with (subscript L) and without NIR irradiation. n.d. means non detected. Bars represent the mean \pm SEM of triplicate experiments.

In order to address the effect of enzymatic activity and laser irradiation on the anticancer property of graphene platforms CCK8 assay was performed. HeLa cells were treated with graphene derivatives for 48 hours. NIR irradiated nG-Trz with loaded doxorubicin showed concentration and irradiation dependence therapeutic efficiency. nG_{DOX}-G-M was more toxic than nG-G-M (without doxorubicin), proving the synergistic effect of chemotherapy and enzyme catalyzed cascade reactions on the anticancer activity of graphene platforms.

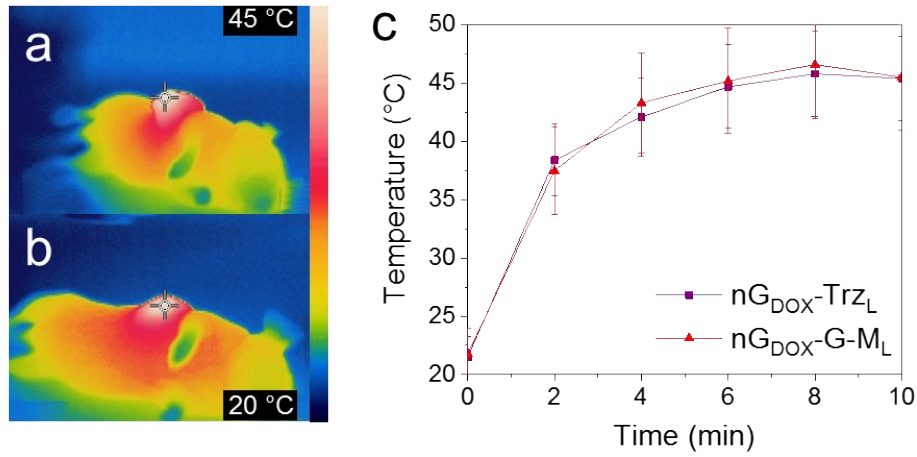


Figure S14. Exemplary thermographic images of tumor-bearing nude mice after treatment with (a) nG_{DOX}-Trz_L and (b) nG_{DOX}-G-M_L. The maximum temperature of ~45 °C was reached after 4 minutes of NIR irradiation. c) Temperature vs. time curves of tumor irradiation by laser.

To calculate photothermal conversion rate (η), the following equation was used^[9]:

$$\eta = \frac{(C_T M_T + C_{nG} M_{nG}) \Delta T}{I A \Delta t}$$

where C_T ,^[10] C_{nG} ^[11] – specific heat of tumors and graphene materials, M_T ,^[12] M_{nG} – mass of tumors and graphene materials, ΔT – temperature rise, Δt – time interval, I – laser intensity, A – illumination area. Assuming that the ratio of $C_{nG} * M_{nG} / C_T * M_T \sim 0$, $C_T = 3.8 \text{ J/g} * \text{K}$, $M_T = 1 \text{ g}$, $I = 1 \text{ W/cm}^2$, $A = 1 \text{ cm}^2$, the values of photothermal conversion rate are listed in Table S4.

Table S4. Values of photothermal conversion rate from time.

Time	η
2 min	0.57
4 min	0.37
6 min	0.27
8 min	0.21
10 min	0.16

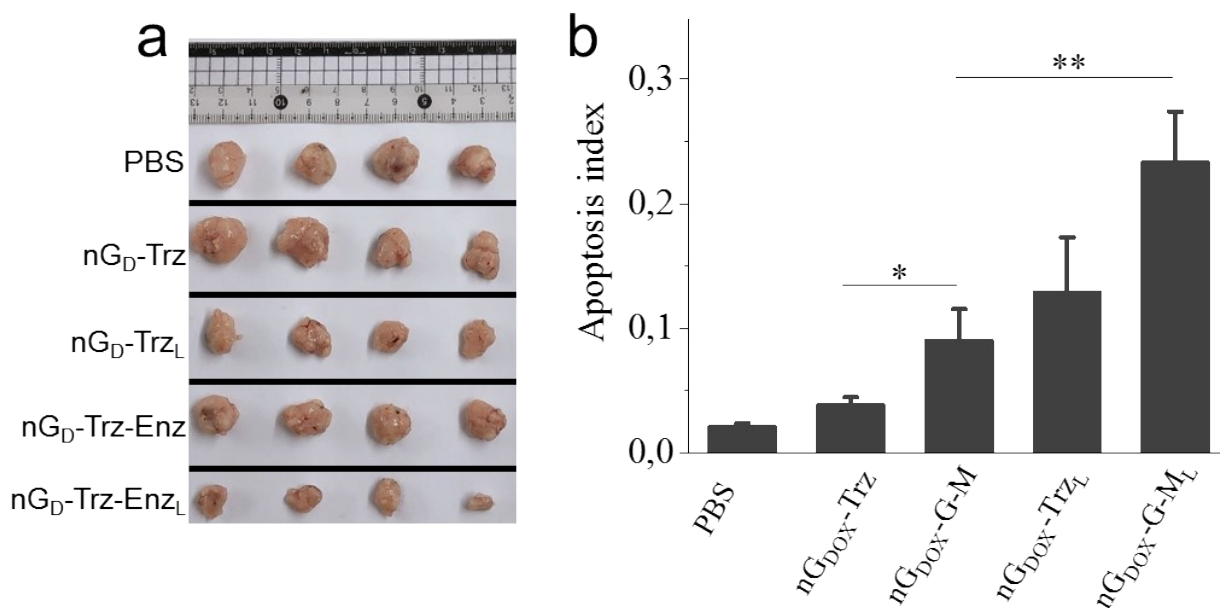


Figure S15. a) Photograph of excised solid tumor tissues of all the mice in each group. b) The apoptosis index was calculated as a ratio of TUNEL-positive cells in DAPI-positive cells counted by ImageJ.

References

- 1 J. Stöhr, *Principles, Techniques, and Instrumentation of NEXAFS*, **1992**, Springer Berlin Heidelberg: Berlin, Heidelberg.
- 2 P. E. Batson, *Phys. Rev. B* **1993**, *48*, 2608.
- 3 B. Schlüter, R. Mülhaupt, A. Kailer, *Tribol. Lett.* **2013**, *53*, 353-363.
- 4 C. Ehlert, W. E. S. Unger, P. Saalfrank, *Phys. Chem. Chem. Phys.* **2014**, *16*, 14083.
- 5 C. Ehlert, *Doctoral Thesis*, University Potsdam, **2016**, <https://publishup.uni-potsdam.de/frontdoor/index/index/docId/10484>.
- 6 G. Geday, I. S. Donskyi, M. F. Gholami, G. Algara-Siller, F. Witte, A. Lippitz, W. E. S. Unger, B. Paulus, J. P. Rabe, M. Adeli, R. Haag, *Small* **2019**, *15*, 1805430.
- 7 A. Faghani, I. S. Donskyi, M. F. Gholami, B. Ziem, A. Lippitz, W. E. S. Unger, C. Böttcher, J. P. Rabe, R. Haag, M. Adeli, *Angew. Chem. Int. Ed.* **2017**, *56*, 2675-2679.

- 8 Y. Zubavichus, A. Shaporenko, M. Grunze, M. Zharnikov, *J. Phys. Chem. B* **2008**, *112*, 4478-4480.
- 9 H. Zhang, H.J. Chen, X. Du, D. Wen, *Solar Energy*, **2014**, *100*, 141-147.
- 10 K. Giering, I. Lamprecht, O. Minet, A. Handke, *Thermochimica Acta*, **1995**, *251*, 199-205.
- 11 Q.-Y. Li, K. Xia, J. Zhang, Y. Zhang, Q. Li, K. Takahashi, X. Zhang, *Nanoscale*, **2017**, *9*, 10784-10793.
- 12 U. D. Monte, *Cell Cycle*, **2009**, *8*, 505-506.